



Missouri University of Science and Technology  
**Scholars' Mine**

---

Electrical and Computer Engineering Faculty  
Research & Creative Works

Electrical and Computer Engineering

---

01 Jan 2004

## Robust Near-Field Adaptive Beamforming with Distance Discrimination

Y. Rosa Zheng

Missouri University of Science and Technology, [zhengyr@mst.edu](mailto:zhengyr@mst.edu)

M. El-Tanany

R. A. Goubran

Follow this and additional works at: [https://scholarsmine.mst.edu/electrical\\_and\\_computer\\_engineering\\_facwork](https://scholarsmine.mst.edu/electrical_and_computer_engineering_facwork)

 Part of the [Electrical and Computer Engineering Commons](#)

---

### Recommended Citation

Y. R. Zheng et al., "Robust Near-Field Adaptive Beamforming with Distance Discrimination," *IEEE Transactions on Speech and Audio Processing*, Institute of Electrical and Electronics Engineers (IEEE), Jan 2004.

The definitive version is available at <https://doi.org/10.1109/TSA.2004.832982>

This Article - Journal is brought to you for free and open access by Scholars' Mine. It has been accepted for inclusion in Electrical and Computer Engineering Faculty Research & Creative Works by an authorized administrator of Scholars' Mine. This work is protected by U. S. Copyright Law. Unauthorized use including reproduction for redistribution requires the permission of the copyright holder. For more information, please contact [scholarsmine@mst.edu](mailto:scholarsmine@mst.edu).

# Robust Near-Field Adaptive Beamforming With Distance Discrimination

Yahong Rosa Zheng, Rafik A. Goubran, *Member, IEEE*, and Mohamed El-Tanany

**Abstract**—This paper proposes a robust near-field adaptive beamformer for microphone array applications in small rooms. Robustness against location errors is crucial for near-field adaptive beamforming due to the difficulty in estimating near-field signal locations especially the radial distances. A near-field regionally constrained adaptive beamformer is proposed to design a set of linear constraints by filtering on a low rank subspace of the near-field signal over a spatial region and frequency band such that the beamformer response over the designed spatial-temporal region can be accurately controlled by a small number of linear constraint vectors. The proposed constraint design method is a systematic approach which guarantees real arithmetic implementation and direct time domain algorithms for broadband beamforming. It improves the robustness against large errors in distance and directions of arrival, and achieves good distance discrimination simultaneously. We show with a nine-element uniform linear array that the proposed near-field adaptive beamformer is robust against distance errors as large as  $\pm 32\%$  of the presumed radial distance and angle errors up to  $\pm 20^\circ$ . It can suppress a far field interfering signal with the same angle of incidence as a near-field target by more than 20 dB with no loss of the array gain at the near-field target. The significant distance discrimination of the proposed near-field beamformer also helps to improve the dereverberation gain and reduce the desired signal cancellation in reverberant environments.

**Index Terms**—Dereverberation, distance discrimination, interference suppression, microphone array, near-field beamforming, regionally constrained beamforming, robust adaptive beamforming, robustness against location errors.

## I. INTRODUCTION

IT IS WELL KNOWN that dynamically adaptive beamformers can achieve better performance than fixed-weight beamformers of comparable sizes when background noises and interference are time-varying or their locations and statistics are unknown [1, p. 349]. Unfortunately, adaptive beamformers suffer from performance degradation when there are signal steering errors and other array imperfections [1]–[3]. The problem of array's sensitivity to signal location errors becomes more pronounced in near-field adaptive beamforming than

in conventional far field beamforming, because the three-dimensional (3-D) near-field signal location is more difficult to estimate than the two-dimensional (2-D) direction of arrival (DOA) in far field cases. The accuracy in distance estimation is particularly low [4] resulting in unacceptable performance of near-field adaptive beamformers. As a rule of thumb, near-field beamforming is required to avoid severe performance degradation when the signals are located within the radial distance of  $R_a^2/\lambda$ , where  $R_a$  is the size of the array and  $\lambda$  is the wavelength of the operating frequency [5], [6]. These situations arise, for example, in applications of microphone arrays in small rooms and automobiles which involve time-varying signals and fast changing environment. Consequently, robust techniques that can tolerate large distance and DOA errors are required for near-field adaptive beamforming.

Currently, research on near-field adaptive beamforming remains very scarce in the array processing literature. The majority of near-field beamforming techniques are fixed-weight or “statically” adaptive beamforming methods which are either designed for specified beamformer responses [6]–[8] or optimized for certain noise and interference environment [9]–[12]. To be adaptive to the changing environment encountered by near-field beamforming applications, one approach is the two-mode method proposed in [10]. This method first gathers information on the acoustical environment and adapts the beamformer weights to the gathered data, then uses the obtained weights “statically” in the actual operation mode. It has been used in hands-free speech pickup in moving vehicles with some performance improvement over fixed-weight beamformers. However, frequent offline calibration is required to account for the changing environment. An alternative approach is the two-stage method [13], [14] which uses several fixed-weight near-field beamformers in the first stage to focus on the desired and interfering signals. It then employs a standard adaptive noise canceller in the second stage to adaptively suppress the noise and interference. The two-stage system is certainly more complex than a single stage adaptive beamformer and it requires the absence of the desired signal during data adaptation. Thus a voice activity detector (VAD) is required and a nonideal VAD will degrade the performance of the two-stage system substantially. In both approaches, the weight vectors of the near-field beamformers remain fixed during their operation.

To the best of our knowledge, there has been no report on dynamically adaptive near-field beamformers due to the robustness problem. The large number of research papers on robust adaptive beamforming deal with the far field case only (see [15] and the references therein for a thorough review of this area). Within these far field robust adaptive beamforming techniques,

Manuscript received August 29, 2003; revised April 2, 2004. This work was supported by Natural Sciences and Engineering Research Council (NSERC) of Canada, and in part by Communications and Information Technology Ontario (CITO) and Mitel Networks, Inc., Canada. The guest editor coordinating the review of this manuscript and approving it for publication was Dr. Man Mohan Sondhi.

Y. R. Zheng is with the Department of Electrical and Computer Engineering, University of Missouri-Columbia, Columbia, MO 65211 USA (e-mail: zhengyr@missouri.edu).

R. A. Goubran and M. El-Tanany are with the Department of Systems and Computer Engineering, Carleton University, Ottawa, ON K1S 5B6 Canada (e-mail: goubran@sce.carleton.ca, tanany@sce.carleton.ca).

Digital Object Identifier 10.1109/TSA.2004.832982

several approaches have been developed for robustness against location errors. These include linearly constrained minimum variance (LCMV) beamforming [16]–[20], eigenspace-based beamforming [21], [22], diagonal loading [2], [23], [24] or quadratically constrained beamforming [25], [26], and other nonlinearly constrained beamforming [27]–[29]. The LCMV approach is the most commonly used adaptive beamforming method. Robust LCMV methods utilize linear constraints to control the beamformer's power response [16]–[19] or the power response of the spatial blocking filter [20] of the generalized sidelobe canceller (GSC) structure. The robustness against location error is achieved by reduced sensitivity in the look direction via eigenvector constraints [16]–[18] or derivative constraints [19], [20]. Eigenspace-based beamforming and diagonal loading methods are known to provide robustness against location errors as well as other types of array mismatches [23]. They have been developed for far field narrow band signal sources using both linear constraints and quadratic constraints. Soft quadratic constraints have also been used in [25] to trade off robustness against location errors and degradation on beamformer responses. Among the nonlinearly constrained robust adaptive beamforming methods, Sondhi and Elko [27] have used fourth-order constraints to enable a gradient search algorithm. Hoshuyama *et al.* [28] have taken an extraordinary approach which employs nonlinearly constrained adaptive spatial blocking filters and a norm-constrained sidelobe canceller in the GSC structure. With a very small linear array of only four elements, this approach achieves outstanding robustness against the target direction error as large as  $\pm 20^\circ$  with steep transitions from the desired region to the interference region. This method has been reformulated by [29] into frequency domain implementation. In principle, all of these far field robust adaptive beamforming methods have the potential of being extended to or modified for near-field adaptive beamforming. However, their effectiveness in near-field adaptive beamforming has not been investigated.

In this paper, we propose a regionally constrained beamforming method for near-field robust adaptive beamformer design. We extend the idea of the far field eigenvector constrained LCMV beamforming [3], [16] to the near-field scenario. The reason for choosing the eigenvector constrained LCMV method is that we are able to establish a direct relationship between the desired near-field target region and the eigen-structure of a near-field signal distributed over this target region. We show that a low rank subspace representation provides sufficient approximation to the near-field regional signal. By filtering on this signal subspace, the proposed method provides a systematic constraint design which can accurately control the beamformer response over the target region. The beamformer's robustness against location errors is then achieved via unit gain constraints over the target region. The advantages of the proposed method are its robustness against large errors in distance as well as in DOAs, and its direct and effective control over a specified region. Similar to the far field eigenvector constraint method, the near-field regionally constrained adaptive beamformer is also a direct time domain method for broadband beamforming which guarantees dynamic adaptation using standard iterative algorithms. It can efficiently utilize the array's degrees of freedom

with real arithmetic implementation, thus the complexity of the beamformer is significantly reduced.

Another advantage of the proposed near-field beamformer is its capability in distance discrimination. Many existing near-field beamforming methods, either fixed-weight or statically adaptive, emphasize only on improving the array response and array gain for near-field signals [6]–[12], [30]. The potential of distance discrimination of near-field beamforming has not been fully exploited. Distance discrimination is the capability of near-field beamforming to discriminate signals with the same angle of incidence but originating from different distances [31]. This scenario arises when a strong wall reflection or noise source originates from a location behind a desired near-field signal. The simplified far field beamforming method has no means of separating them. Ryan and Goubran [31] have shown that enforcing a null constraint on the interference location reduces the array gain and robustness. They proposed a method of imposing a soft null constraint on the far field interference to trade off the far field interference reduction and the array gain at the near-field focal point. With the proposed beamformer in this paper, better distance discrimination is achieved inherently with the regional constraints designed for robust beamforming. The proposed beamformer can simultaneously improve the distance discrimination and the robustness against location errors without additional constraints. It can effectively and adaptively suppress far field interference with the same angle of incidence as the desired signal, and the desired near-field signal is preserved with no loss of array gain.

The performances of the proposed near-field adaptive beamformer will be evaluated in Section IV in terms of its robustness against location errors, distance discrimination, interference suppression, and dereverberation. We show, using the example of a nine-element uniform linear array, that the proposed near-field robust adaptive beamformer can tolerate a distance error as large as  $\pm 32\%$  of the presumed radial distance and a DOA error as large as  $\pm 20^\circ$ . Its robustness against DOA errors is comparable to the existing far field robust adaptive beamforming schemes. Its robustness against distance errors cannot be achieved by far field beamforming and has not been reported by other near-field beamforming methods. Its distance discrimination is significant. When the constrained region is properly designed, the proposed near-field adaptive beamformer can obtain more than 15 dB attenuation outside the constrained distance range. Its capability of uncorrelated interference suppression is demonstrated via simulation examples that involves far field interference from the same DOA as the desired signal but at different distances. The proposed beamformer can suppress the near or far field interfering signals by more than 20 dB. For applications in reverberant environments, the proposed near-field adaptive beamforming method is applied to a nested linear array [14] consisting of seventeen elements which is subbanded into three subarrays for the speech frequency band [300, 3400] Hz. The compound array achieves good de-reverberation gain of 5 to 7 dB in the two lower subbands. Only a slight signal cancellation of 3.0 dB occurs in the high subband which is hardly noticeable in subjective listening tests. The overall quality of the array output is improved over the reverberant speech.

## II. NEAR-FIELD ADAPTIVE BEAMFORMING

Consider a broadband array beamformer with  $M$  elements and  $K$  taps attached at each element. The elements of the array are located at  $\{\mathbf{x}_m = (r_m, \theta_m, \phi_m), m = 1, 2, \dots, M\}$  in a spherical coordinate system, where  $r_m$ ,  $\theta_m$ , and  $\phi_m$  denote the radial distance, azimuth angle and elevation angle, respectively. Without loss of generality, the coordinate system is defined such that its origin is at the phase center of the array. If the signal target is located at  $\mathbf{x}_s = (r_s, \theta_s, \phi_s)$  with  $r_s < R_a^2/\lambda$ , where  $R_a$  is the largest array dimension and  $\lambda$  is the operating wavelength, then the near-field propagation model is required and the near-field steering vector of the array beamformer is defined as [1]

$$\mathbf{a}(\mathbf{x}_s, f) = \frac{r_s}{e^{j2\pi f r_s/c}} \left[ \frac{e^{j2\pi f r_{1s}/c}}{r_{1s}}, \dots, \frac{e^{j2\pi f (r_{ms}/c - k)}}{r_{ms}}, \dots, \frac{e^{j2\pi f (r_{Ms}/c - K + 1)}}{r_{Ms}} \right]^T \quad (1)$$

where the superscript  $(\cdot)^T$  represents transpose, and  $f$  is the frequency,  $c$  is the propagation speed,  $r_s = |\mathbf{x}_s|$  and  $r_{ms} = |\mathbf{x}_m - \mathbf{x}_s|$  are the distances from the signal source to the phase center of the array and the  $m$ th element, respectively. Let the input vector of the array beamformer be the concatenated snapshot samples grouped into an  $N$ -dimensional ( $N = MK$ ) vector denoted as  $\mathbf{u}(k)$ , where  $k$  is the time instance. The beamformer output  $y(k)$  can be expressed in matrix form [3] as  $y(k) = \mathbf{w}^H \mathbf{u}(k)$ , where  $\mathbf{w}$  is the concatenated weight vector of the beamformer, and the superscript  $(\cdot)^H$  represents complex conjugate transpose. Using the LCMV method, the near-field adaptive beamformer tries to minimize the output power subject to some constraints. That is

$$\min_{\mathbf{w}} \quad \{\mathbf{w}^H \mathbf{R}_{uu} \mathbf{w}\} \quad (2)$$

$$\text{subject to} \quad \mathbf{C}^H \mathbf{w} = \mathbf{h} \quad (3)$$

where  $\mathbf{R}_{uu}$  is the  $N \times N$  covariance matrix of the concatenated input vector, i.e.,  $\mathbf{R}_{uu} = E\{\mathbf{u}(k)\mathbf{u}^H(k)\}$  with  $E\{\cdot\}$  being the expectation operator. The matrix  $\mathbf{C}$  is the constraint matrix and  $\mathbf{h}$  is the desired response vector. If the dimension of  $\mathbf{C}$  is  $N \times L$ , then (3) is a set of  $L$  linear constraint equations controlling the beamformer response.

The optimal solution to the constrained minimization problem is well-known [3]

$$\mathbf{w}_{opt} = \mathbf{R}_{uu}^{-1} \mathbf{C} (\mathbf{C}^H \mathbf{R}_{uu}^{-1} \mathbf{C})^{-1} \mathbf{h}. \quad (4)$$

The optimal weight vector  $\mathbf{w}_{opt}$  can be decomposed into two orthogonal components: a fixed beamformer  $\mathbf{w}_q$  and an unconstrained adaptive weight vector  $\mathbf{w}_a$ . They are determined by

$$\mathbf{w}_q = \mathbf{C} (\mathbf{C}^H \mathbf{C})^{-1} \mathbf{h} \quad (5)$$

$$\mathbf{w}_a = (\mathbf{C}_a^H \mathbf{R}_{uu} \mathbf{C}_a)^{-1} \mathbf{C}_a^H \mathbf{R}_{uu} \mathbf{w}_q \quad (6)$$

where  $\mathbf{C}_a$  is termed the signal blocking matrix. It is orthogonal to  $\mathbf{C}$  and satisfies  $\mathbf{C}^H \mathbf{C}_a = \mathbf{0}$ . This decomposition is known as the generalized sidelobe canceller (GSC) [3].

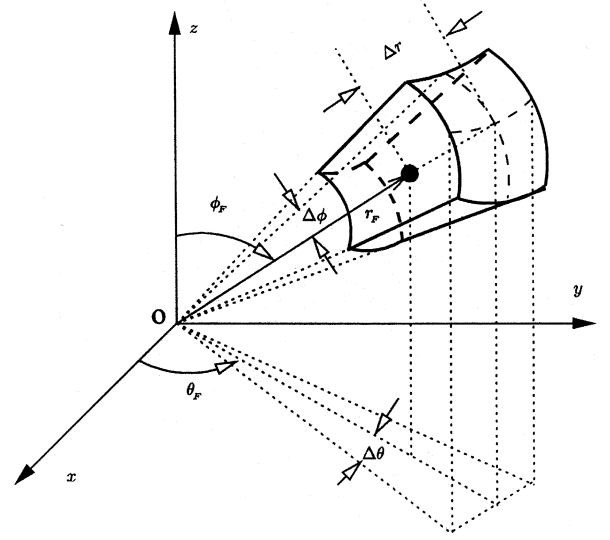


Fig. 1. Constrained spatial region  $\Omega = (\pm \Delta r, \pm \Delta \theta, \pm \Delta \phi)$ . The presumed focal point is  $\mathbf{x}_F = (r_F, \theta_F, \phi_F)$ .

The iterative solution to  $\mathbf{w}_a$  using the normalized least mean square (NLMS) algorithm [1, p. 311], [34, p. 432] is

$$\mathbf{w}_a(k+1) = \mathbf{w}_a(k) + \mu \frac{\mathbf{u}(k)e(k)}{\mathbf{u}^H(k)\mathbf{u}(k)} \quad (7)$$

where  $\mu$  is the step size, and  $e(k)$  is the error defined by  $e(k) = [\mathbf{w}_q - \mathbf{C}_a \mathbf{w}_a]^H \mathbf{u}(k)$ .

This decomposition provides important insights for adaptive beamformer design. Since the fixed beamformer  $\mathbf{w}_q$  is independent of the array input data and it is in the constraint subspace which spans the columns of the constraint matrix  $\mathbf{C}$ , the beamformer response is deterministically controlled by the fixed beamformer  $\mathbf{w}_q$  for the source sample space in the constraint subspace. Selection of constraint equation can be viewed as a deterministic beamformer design problem. For example, a simple point constraint may be chosen as  $\mathbf{C} = \mathbf{a}(\mathbf{x}, f)$  and  $\mathbf{h} = 1$ , which enforces a unit gain response at the location  $\mathbf{x}$  and the frequency  $f$ . Since each column of  $\mathbf{C}$  uses one degree of freedom, efficient utilization of the array's degrees of freedom becomes important for sufficient control of the beamformer response while giving enough degrees of freedom for data adaptation. In Section III, we will first develop a subspace representation for broadband signals over a near-field spatial region, then design our regionally constrained near-field adaptive beamformer through filtering on this subspace.

## III. PROPOSED ROBUST NEAR-FIELD BEAMFORMING

### A. Near-Field Signal Representation

Consider a signal source over a normalized angular frequency band  $B$  and a spatial region  $\Omega = (\pm \Delta r, \pm \Delta \theta, \pm \Delta \phi)$  around the estimated focal point  $\mathbf{x}_F = (r_F, \theta_F, \phi_F)$ , as shown in Fig. 1. Denote the signal source sample vector by  $\mathbf{s}(k)$  and its power

spectrum density by  $S(f)$ . The source sample covariance matrix observed at the array beamformer is

$$\mathbf{R}_{ss} = E\{\mathbf{s}(k)\mathbf{s}^T(k)\} = \frac{1}{\Omega} \frac{1}{B} \int_{\Omega} \int_B S(f) \mathbf{a}(\mathbf{x}, f) \mathbf{a}^H(\mathbf{x}, f) df d\mathbf{x} \quad (8)$$

where  $\mathbf{a}(\mathbf{x}, f)$  is the near-field steering vector defined in (1).

Let the eigenvalues of the covariance matrix  $\mathbf{R}_{ss}$  be  $\lambda_1 > \lambda_2 > \dots > \lambda_N$  and  $\mathbf{v}_1, \mathbf{v}_2, \dots, \mathbf{v}_N$  be the corresponding eigenvectors. The source sample vector  $\mathbf{s}(k)$  can be represented by the discrete Karhunen-Loève expansion [32] as  $\mathbf{s}(k) = \sum_{n=1}^N s_n \mathbf{v}_n$ , where  $s_n = \mathbf{v}_n^T \mathbf{s}(k)$ . Truncating the sum of  $\mathbf{s}(k)$  results in a low rank approximation of the source sample vector

$$\mathbf{s}(k) \approx \hat{\mathbf{s}}(k) = \sum_{n=1}^L s_n \mathbf{v}_n. \quad (9)$$

Equation (9) is the most efficient rank  $L$  representation of the signal source in the second order statistics sense. The eigenvalues  $\lambda_n$  represent the energy of the source sample vector projected onto the basis vectors  $\mathbf{v}_n$ . The representation dimension  $L$  is selected to obtain a required approximation error  $\epsilon(L)$  defined as

$$\begin{aligned} \epsilon(L) &= E\{|\mathbf{s}(k) - \hat{\mathbf{s}}(k)|^2\} \\ &= \sum_{n=L+1}^N \mathbf{v}_n^T \mathbf{R}_{ss} \mathbf{v}_n = \sum_{n=L+1}^N \lambda_n. \end{aligned} \quad (10)$$

For a broadband signal located on a single spatial point, it has been found [33] that the eigenvalues  $\lambda_n$  of the signal decrease rapidly when  $n > \beta$ , where  $\beta = 2BT(\mathbf{x}_s)$ , and  $T(\mathbf{x}_s)$  is the normalized length of the observation time window. For near-field signals impinging on an array, the observation time  $T(\mathbf{x}_s)$  is a function of the source location. It is determined by

$$T(\mathbf{x}_s) = \tau(\mathbf{x}_s) + K - 1 \quad (11)$$

where  $\tau(\mathbf{x}_s) = [\max(r_{ms}) - \min(r_{ms})]/c/F_s$  for  $m = 1, 2, \dots, M$ . Note that  $M$  is the number of array elements,  $K$  is the length of the tapped-delay-line, and  $F_s$  is the sampling frequency.

For a point source, it has been found that over 99.99% of the energy is concentrated in the first  $L = (\beta + 1)$  eigenvalues [16], [33]. For a regional signal source, on the other hand, we find that a much larger  $L$  is required to represent it with the same approximation error. For example, Fig. 2 shows several approximation error curves obtained by a nine-element linear array for signals distributed in different spatial regions  $\Omega$  with  $\Delta r = 0$  and  $\Delta\theta$  varying from  $0^\circ$  to  $20^\circ$ . The array is located along the  $x$ -axis, thus  $\Delta\phi$  does not affect the Karhunen-Loève expansion. The normalized signal bandwidth is  $B = [0.22, 0.44]$ . The elements of the array are uniform with  $\lambda/2$  spacing, where  $\lambda$  is the wavelength of the high frequency edge. The size of the array is  $R_a = 4\lambda$  and the focal point is assumed at  $\mathbf{x}_F = (1.25R_a, 90^\circ, 90^\circ)$ . Each element has  $K = 25$  taps. It is clearly shown that the required number of eigenvalues increases dramatically as the angle  $\Delta\theta$  increases slightly. For the approximation error of  $\epsilon(L) = -40$  dB, a point source (curve A,  $\Delta\theta = 0$ )

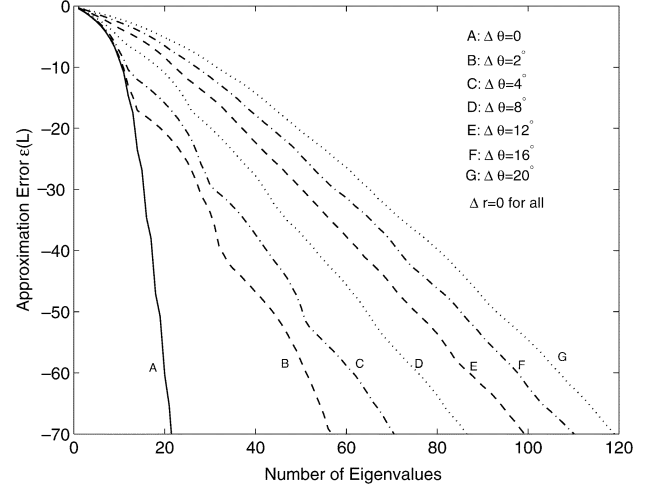


Fig. 2. The Karhunen-Loève representation of a broadband signal source—the approximation error by the first  $L$  eigenvalues.

requires  $L = 19$  largest eigenvalues. If  $\Delta\theta = 2^\circ$ , then  $L$  increases to 34 (curve B). The corresponding  $L$  values for curves C to G are 42, 56, 63, 72, 81, respectively. This is intuitively understandable because the signal energy is not concentrated on a point but spread out over the entire region. For a fixed  $\Delta\theta$ , changing  $\Delta r$  also changes the eigen-structure and the approximation error curve. The eigenvalue distribution of the covariance matrix depends not only on the bandwidth  $B$  and the length of the tapped-delay-line  $K$ , but also on the location, size, and shape of the spatial region  $\Omega$ .

The implications from Fig. 2 are a low rank subspace of a signal source can be used efficiently to represent the signal source, hence, it is sufficient to control the beamformer response by filtering on this subspace through the constraint equations; although a regional source requires much larger number of eigenvalues than a point source, its low rank approximation still provide great savings in the degrees of freedom in controlling the beamformer response.

### B. Near-Field Regionally Constrained Adaptive Beamforming

Based on the Karhunen-Loève expansion of the near-field signal source described in Section III-A, we are now ready to present the constraint design method for the proposed regionally constrained near-field adaptive beamformer. Assume a flat spectrum of the signal source within the frequency band  $B$ . Then the covariance matrix  $\mathbf{R}_{ss}$  defined in (8) can be computed numerically

$$\mathbf{R}_{ss} = \frac{1}{P} \sum_{i=1}^I \sum_{j=1}^J \mathbf{a}(\mathbf{x}_i, f_j) \mathbf{a}^H(\mathbf{x}_i, f_j) = \frac{1}{P} \mathbf{A} \mathbf{A}^T \quad (12)$$

where  $P = IJ$ , and  $\mathbf{A}$  is a real matrix formed by selecting  $I$  points in the spatial region  $\Omega$  and  $J$  points in the frequency band  $B$

$$\mathbf{A} = [\mathbf{a}_c(\mathbf{x}_1, f_1), \dots, \mathbf{a}_c(\mathbf{x}_i, f_j), \dots, \mathbf{a}_c(\mathbf{x}_I, f_J) | \mathbf{a}_s(\mathbf{x}_1, f_1), \dots, \mathbf{a}_s(\mathbf{x}_i, f_j), \dots, \mathbf{a}_s(\mathbf{x}_I, f_J)] \quad (13)$$

here  $\mathbf{a}_c(\mathbf{x}_i, f_j)$  and  $\mathbf{a}_s(\mathbf{x}_i, f_j)$  are, respectively, the real and imaginary part of the steering vector  $\mathbf{a}(\mathbf{x}_i, f_j)$  at the point  $(\mathbf{x}_i, f_j)$  defined in (1).

Meanwhile, the beamformer responses at these  $P$  points can be controlled by defining the constraint equation as

$$\mathbf{A}^T \mathbf{w} = \mathbf{g} \quad (14)$$

where  $\mathbf{g}$  is the desired response vector defined by

$$\mathbf{g} = [g_{11} \cos(2\pi f_1 \tau_1), \dots, g_{IJ} \cos(2\pi f_J \tau_I), \\ |g_{11} \sin(2\pi f_1 \tau_1), \dots, g_{IJ} \sin(2\pi f_J \tau_I)]^T \quad (15)$$

and  $\tau_i$  is the group delay of the signal location  $\mathbf{x}_i$  relative to the array coordinate origin and  $g_{ij}$  are the desired amplitude responses. Unit gain response is enforced by setting  $g_{ij} = 1$ , and the group delays  $\tau_i$  to the temporal center of the beamformer. The formulation of the matrix  $\mathbf{A}$  and the vector  $\mathbf{g}$  guarantees that the resulting beamformer is implemented by real arithmetic. Besides, the beamformer is internally steered to the focal region by the group delays. Thus no presteering is required and its associated presteering errors are reduced.

To efficiently utilize the degrees of freedom available in the adaptive beamformer, the low rank representation of  $\mathbf{R}_{ss}$  is computed through the singular value decomposition (SVD) [34, p516] of the matrix  $\mathbf{A}$

$$\mathbf{A} = \mathbf{V} \mathbf{\Sigma} \mathbf{U}^T \quad (16)$$

where  $\mathbf{\Sigma}$  is the diagonal matrix containing all singular values  $\sigma_1, \sigma_2, \dots, \sigma_N$  of  $\mathbf{A}$  in descending order. The columns of  $\mathbf{V}$  and  $\mathbf{U}$  are the corresponding singular vectors. The singular values of  $\mathbf{A}$  are related with the eigenvalues of  $\mathbf{R}_{ss}$  by  $\lambda_n = \sigma_n^2 / P$  for  $n = 1, 2, \dots, N$ . Therefore, a rank  $L$  representation of  $\mathbf{R}_{ss}$  corresponds to a rank  $L$  approximation of  $\mathbf{A}$ . That is

$$\mathbf{A} \approx \mathbf{A}_L = \mathbf{V}_L \mathbf{\Sigma}_L \mathbf{U}_L^T \quad (17)$$

where  $\mathbf{\Sigma}_L = \text{diag}\{\sigma_1, \sigma_2, \dots, \sigma_L\}$ . The columns of  $\mathbf{V}_L$  and  $\mathbf{U}_L$  are, respectively, the  $L$  columns of  $\mathbf{V}$  and  $\mathbf{U}$  corresponding to these  $L$  singular values.

Replacing the matrix  $\mathbf{A}$  in (14) by its rank  $L$  approximation (17) yields  $\mathbf{V}_L^T \mathbf{w} = \mathbf{\Sigma}_L^{-1} \mathbf{U}_L^T \mathbf{g}$ . An efficient design of constraint equation  $\mathbf{C}^T \mathbf{w} = \mathbf{h}$  is readily obtained as

$$\mathbf{C} = \mathbf{V}_L \\ \mathbf{h} = \mathbf{\Sigma}_L^{-1} \mathbf{U}_L^T \mathbf{g}. \quad (18)$$

The complete design procedures of the proposed regionally constrained near-field adaptive beamformer are summarized as follows.

- 1) Select a large number of points  $I$  and  $J$  in a specified constraint region  $\Omega$  and frequency band  $B$ , respectively; Form the matrix  $\mathbf{A}$  as in (13) and the desired response vector  $\mathbf{g}$  as in (15);
- 2) Perform the singular value decomposition (SVD) of  $\mathbf{A}$ . Find the matrices  $\mathbf{V}$ ,  $\mathbf{\Sigma}$ , and  $\mathbf{U}$  as in (16);
- 3) Specify an approximation error  $\epsilon(L)$ . For example, an error level of  $-40$  dB is sufficient for unit gain constraints. Then find the required number of constraints  $L$  by computing the approximation error as in (10);

- 4) Form  $\mathbf{\Sigma}_L$ ,  $\mathbf{V}_L$ , and  $\mathbf{U}_L$  by choosing the largest  $L$  singular values in  $\mathbf{\Sigma}$  and the corresponding  $L$  column vectors in  $\mathbf{V}$  and  $\mathbf{U}$ , respectively;
- 5) Compute the linear constraints  $\mathbf{C}$  and  $\mathbf{h}$  as in (18);
- 6) To implement the adaptive beamformer in the GSC structure, compute  $\mathbf{w}_q$  as in (5) and  $\mathbf{w}_a$  as in (6) or (7).

For better numerical precisions, the number of points  $P = IJ$  may be chosen very large. However, we found that the number of constraints  $L$  does not increase with  $P$ . It only depends on the spatial region  $\Omega$ , the frequency band  $B$ , the focal point location  $\mathbf{x}_F$ , the geometry of the array, and the number of taps  $K$  in the tapped-delay-line. Moreover, since constraint design is always done offline, the computational complexity associated with a large  $P$  does not affect the computational complexity and the convergence rate of the resulting adaptive beamformer. They depend mainly on the number of constraints  $L$  and the degrees of freedom for data adaptation  $N - L$ . Through the most efficient low rank approximation, the proposed design method uses the smallest number of constraints  $L$  to achieve sufficient control over the specified region. Consequently, the total degrees of freedom  $N$  can be selected smaller than point-constrained beamformers and it results in better computational efficiency.

The proposed constraint design method for robust near-field beamforming is a direct extension of the far field eigenvector constrained LCMV beamforming proposed in [16]. It is not only suitable for controlling the beamformer response for a robust adaptive beamformer, but also effective for designing a fixed near-field beamformer. If we choose  $L = N$ , the constraint matrix uses all degrees of freedom, then a fixed beamformer results. Some weighting functions, such as the Chebyshev function may be used to shape the beamformer response in both the frequency band and the spatial region. This is analogous to the weighting window method of finite impulse response (FIR) filter design [35], which is applied simultaneously in the frequency domain and 3-D space domain in the near-field beamformer design.

#### IV. PERFORMANCE EVALUATION

Adaptive beamformers are evaluated in terms of the beamformer response, the output signal-to-interference-and-noise ratio (SINR), the array gain, the array sensitivity, and the white noise gain. The beamformer response is defined as [3]

$$b(\mathbf{x}_s, f) = \mathbf{w}^H \mathbf{a}(\mathbf{x}_s, f). \quad (19)$$

It is a function of the spatial point  $\mathbf{x}_s$  and the normalized frequency  $f$ . Array beampattern is the squared magnitude response of the beamformer given by  $|b(\mathbf{x}_s, f)|^2$ .

The output SINR is determined by

$$\text{SINR} = \frac{\mathbf{w}^H \mathbf{R}_{ss} \mathbf{w}}{\mathbf{w}^H \mathbf{R}_{i+n} \mathbf{w}} \quad (20)$$

where  $\mathbf{R}_{i+n}$  is the covariance matrix of the interference and noise. Array gain is the improvement in SINR due to beamforming. It is the ratio of the beamformer output SINR to the input SINR. Array gain sensitivity is the array gain due to signal mismatches normalized with respect to the array gain at the focal point [2].

The white noise gain is a robustness measure of adaptive beamformers. It is defined as the inverse of the  $L_2$  norm of the weight vector [2]

$$G_w = \frac{1}{\mathbf{w}^H \mathbf{w}} \leq M. \quad (21)$$

It is bounded by the number of array elements  $M$ . A small  $G_w$  corresponds to a super-gain or super-directive beamformer [8]. However if the white noise gain is too small, the beamformer is ill-conditioned and the robustness of the beamformer is poor.

#### A. Array Gain Sensitivity

First, the array gain sensitivity of the proposed adaptive beamformer is compared with a near-field fixed beamformer and a near-field point-constrained adaptive beamformer. Comparison to other robust adaptive beamforming methods are also included. The example of a nine-element microphone array is used to illustrate the performances of the proposed near-field regionally constrained adaptive beamformer. The normalized frequency band of interest is  $B = [0.22, 0.44]$ . Each element has  $K = 25$  taps. The array elements are uniformly placed along the  $x$  axis with  $\lambda/2$  spacing, where  $\lambda$  is the wavelength of the high frequency edge of the frequency band. Thus the size of the array was  $R_a = 4\lambda$ . The presumed focal point was well within the near-field of the array at  $\mathbf{x}_F = (r_F, \theta_F, \phi_F) = (5\lambda, 90^\circ, 90^\circ)$ .

The near-field regionally constrained adaptive beamformer was designed using the proposed method outlined in Section III-B. The constrained frequency band was  $B$  and the constrained region  $\Omega$  was chosen as  $\Delta r = 0.1r_F$ ,  $\Delta\theta = 4^\circ$  and  $\Delta\phi = 0$ . The linear array located along the  $x$ -axis has no resolution on the elevation angle  $\phi$ . Thus  $\Delta\phi$  does not affect the constraint design. The resulting constraints used  $L = 78$  degrees of freedom of the beamformer. Thus the adaptive beamformer had 147 degrees of freedom for dynamic adaptation. A near-field point-constrained adaptive beamformer was designed using the eigenvector constraint method [16]. It used  $L = 18$  constraint vectors to ensure unit gain at the focal point and over the frequency band. A near-field fixed beamformer was also designed by optimization under the far field spherically isotropic noise field [31]. It was designed to focus at the same focal point as the adaptive beamformers. Its weights remained unchanged after the optimization.

The array gain sensitivity of the three beamformers were evaluated as functions of source locations, shown in Fig. 3. The array gain sensitivity as a function of the radial distance is plotted in Fig. 3(a). It is a measure of robustness against location error as well as the capability of distance discrimination of near-field beamformers. The solid line shows that the point-constrained adaptive beamformer is very sensitive to distance errors. It has strong capability of discriminating signals located at different distances along the same direction as the desired signal. The dash-dot line shows that the regionally constrained beamformer was able to maintain unit gain in the constrained range of  $[0.9r_F, 1.1r_F]$ . Meanwhile, it achieved 15 dB attenuation at distances outside the range of  $[0.5r_F, 2.0r_F]$ . This means that the proposed beamformer has greatly improved robustness against distance error while maintaining sufficient

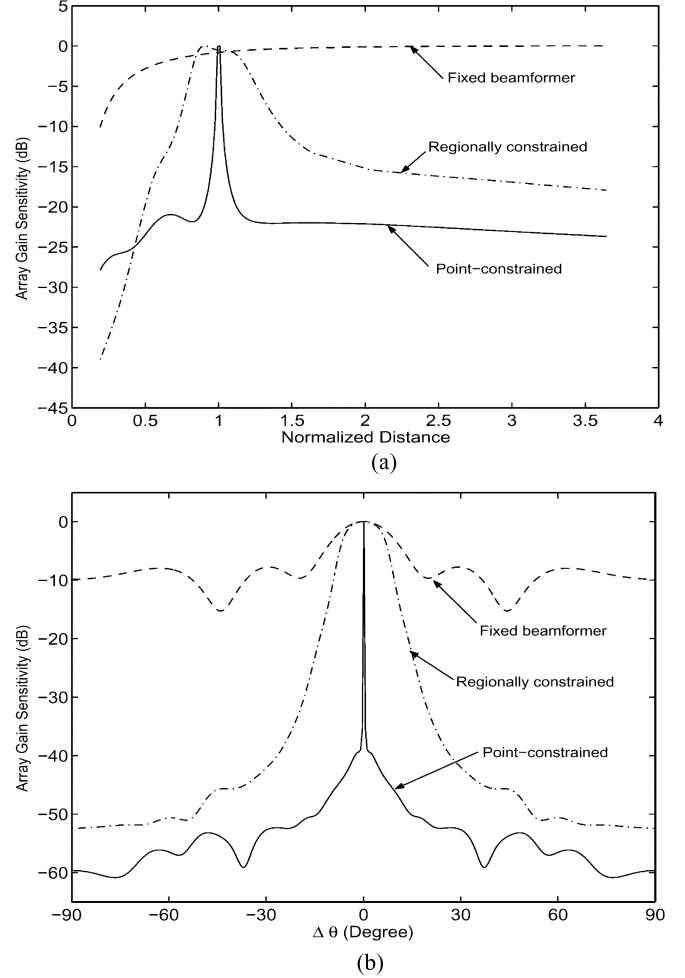


Fig. 3. Array gain sensitivity as functions of the source location. All three beamformers have nine equi-spaced elements covering the frequency band  $B = [0.22, 0.44]$ . The size of the arrays is  $4\lambda$  and the focal point is  $\mathbf{x}_F = (5\lambda, 90^\circ, 90^\circ)$ , with  $\lambda$  being the wavelength of the high frequency edge. The regionally constrained beamformer is designed with  $\Delta r = 0.1r_F$  and  $\Delta\theta = 4^\circ$ . Distances are normalized with respect to  $r_F$ . (a) Distance discrimination, evaluated at  $\theta = \theta_F$ . (b) Robustness against DOA error, evaluated at  $r = r_F$ .

distance discrimination outside the target region. In comparison, the dashed line shows that the fixed beamformer is robust but has no advantage in distance discrimination.

The array gain sensitivity versus the DOA  $\theta$  is plotted in Fig. 3(b) with the radial distance  $r = r_F$ . The point-constrained adaptive beamformer had a very sharp spike at the look direction, as shown by the solid line. A small DOA error would result in dramatic reduction of the array gain to below  $-40$  dB. Its robustness against DOA error is clearly very poor. In comparison, the proposed regionally constrained adaptive beamformer maintained a high array gain in the target DOA region of  $\pm 4^\circ$  while achieving strong attenuation outside the target region. The fixed beamformer, on the other hand, is very robust against the DOA error. However, it does not provide adequate attenuation outside the target region.

It is noted that our near-field adaptive beamformer achieves similar robustness against DOA error as the far field robust adaptive beamformer proposed in [28]. Compared to curve D in Fig. 4 of [28] obtained by a four-element uniform array using

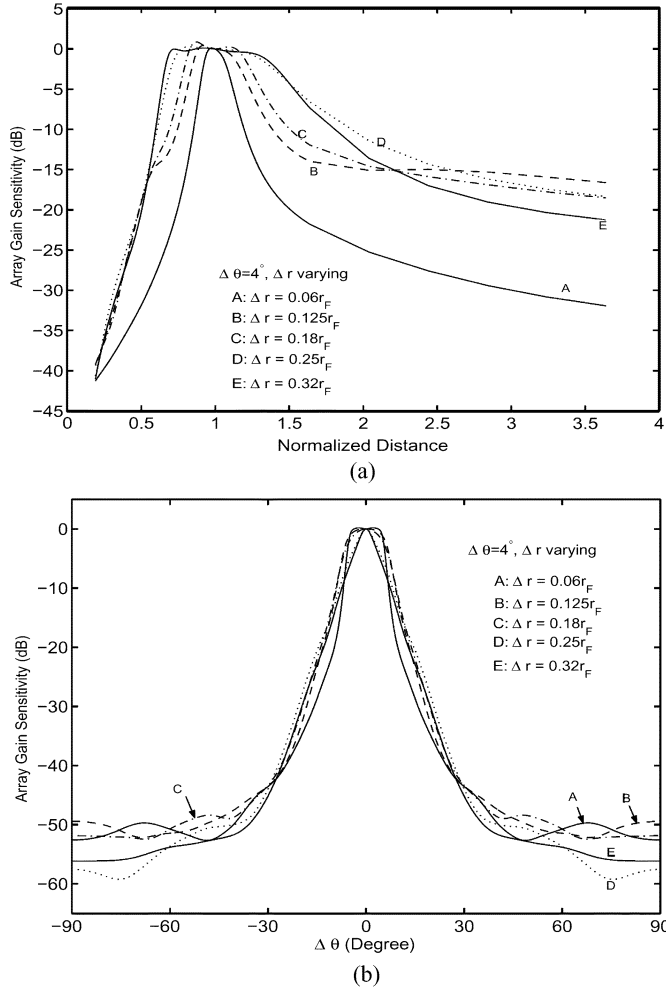


Fig. 4. Array gain sensitivity for different allowable location errors in distances. The constrained region has a fixed  $\Delta\theta$  and varying  $\Delta r$ . (a) Distance discrimination, evaluated at  $\theta = \theta_F$ . (b) Robustness against DOA error, evaluated at  $r = r_F$ .

far field beamforming techniques, our regionally constrained adaptive beamformer exhibits slightly inferior transitions (not as steep) from the constrained region to the outside of the region, but achieves slightly deeper attenuation when the DOA error is large which means better suppression of the noise and interference from those regions. In addition, our regionally constrained near-field beamformer achieves distance discrimination at the cost of a few more array elements than the far field beamformer which does not have resolution in distance. The curves A and B in Fig. 4 of [28] obtained by the far field fixed beamformer and the point-constrained adaptive beamformer are very similar to the performances of the near-field ones in Fig. 3(b), respectively.

Next, we demonstrate that the proposed adaptive beamformer has accurate and sufficient control over differently constrained regions. As shown in Figs. 4 and 5, the regionally constrained adaptive beamformer were designed for different constrained regions with various values of  $\Delta r$  and  $\Delta\theta$ . All other parameters were the same as those in Fig. 3.

In Fig. 4, all curves had the same constrained angle  $\Delta\theta = 4^\circ$ . The constrained distance  $\Delta r$  increased from  $0.06r_F$  for curve

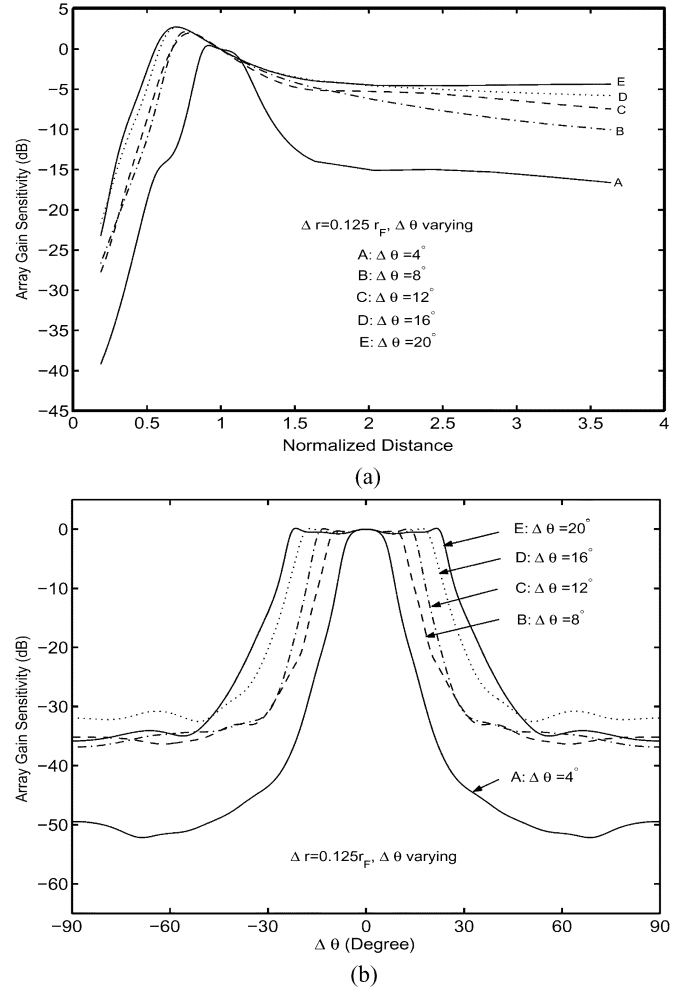


Fig. 5. Array gain sensitivity for different allowable location errors in DOA. The constrained region has a fixed  $\Delta r$  and varying  $\Delta\theta$ . (a) Distance discrimination, evaluated at  $\theta = \theta_F$ . (b) Robustness against DOA error, evaluated at  $r = r_F$ .

A to  $0.32r_F$  for curve E. Fig. 4(a) shows the array gain sensitivity versus distance. Unit gain over the constrained distances was well controlled by the proposed beamformers. The smaller  $\Delta r$  resulted in better attenuation outside the constrained distance. Even with the constrained distance as large as  $\pm 32\%$  of the focal distance  $r_F$ , more than 15 dB attenuation was achieved outside the region of  $[0.5r_F, 2.3r_F]$ . Fig. 4(b) shows the array gain sensitivity versus DOA error. Curves A to C obtained accurate control of unit gain over the  $\pm 4^\circ$  region and deep attenuation outside the constrained region. Curves D and E had slightly reduced gain at the edges of the constrained DOA region. The reduced robustness against DOA error was traded off with their robustness against large distance error  $\Delta r$ . The limitations on the size of constrained regions are due to the size of the array.

In Fig. 5, all curves had the same constrained distance range  $\Delta r = 0.125r_F$ . The constrained angle  $\Delta\theta$  increased from  $4^\circ$  for curve A to  $20^\circ$  for curve E. Fig. 5(a) shows the array gain sensitivity versus distance. Better distance discrimination was achieved when  $\Delta\theta$  was smaller. For a small sized array as the one in this example, constraining over a large DOA region was obtained at the cost of reduced distance discrimination. Fig. 5(b)

shows the array gain sensitivity versus the DOA error. Unit gain over the target angles was well maintained by the designed constraints. The smaller  $\Delta\theta$ , the better attenuation outside the constrained distance. Even with the target DOA region as large as  $\pm 20^\circ$ , strong attenuation of more than 25 dB was achieved outside the constrained region. It is noted that curve A has much deeper attenuation outside the constrained region than the other curves. The exceptional better performance of curve A is due to the match of the constrained region with the capability of the array.

Similar to Fig. 5(b), comparable performance curves were also presented in Fig. 8 of [28] for the far field adaptive beamformer with allowable DOA errors varying from  $4^\circ$  to  $20^\circ$ . Again, steeper transitions were achieved by the far field adaptive beamformer of [28] for all allowable error regions; while the proposed near-field adaptive beamformer obtained slightly better attenuation outside the constrained region with curve A.

The curves in Figs. 4 and 5 provide some insightful guidelines for design trade-offs in choosing the size of the constrained region. Array beamformers have inherent limitations similar to the basic limitations of FIR filters. The smaller the array, the less capable of the beamformer. The farther the focal point away from the array, the less effective the distance discrimination. If the constrained region is too large or the desired response is too stringent, then it will result in an ill-conditioned beamformer weight vector with large  $L_2$  norm and poor robustness. On the other hand, forcing exact responses over the constrained region does not necessarily translate into high SINR at the beamformer output. On contrast, allowing a slightly higher approximation error  $\epsilon(L)$  may free more degrees of freedom for data adaptation. Consequently, interferences and noises can be better suppressed and higher SINR may be obtained.

### B. Performance of Uncorrelated Interference Suppression

Two examples are presented here to elaborate the advantages of the proposed beamformer in robustness against location errors and distance discrimination. The first example compares the robustness of the regionally constrained adaptive beamformer and the point-constrained adaptive beamformer used in Fig. 3. Both beamformers were adapted at the presence of one desired signal  $s_0$  and two interfering signals  $s_1$  and  $s_2$  using the NLMS algorithm. All signals were uncorrelated, band-limited to  $B$ , and with a power of 20 dB above the background noise. The presumed focal point is  $\mathbf{x}_F = (r_F, 90^\circ, 90^\circ)$  for both beamformers. The constrained region of the proposed beamformer is  $\Delta r = 0.1r_F$  and  $\Delta\theta = 4^\circ$ . The desired signal  $s_0$  is off the focal point at  $(0.9r_F, 88^\circ, 90^\circ)$ . The two interfering signals  $s_1$  and  $s_2$  were located at  $(r_F, 50^\circ, 90^\circ)$  and  $(r_F, 120^\circ, 90^\circ)$ , respectively. The converged beamformer responses were then evaluated at several in-band frequencies, as shown in Fig. 6. The beampatterns in Fig. 6(a) shows that the point-constrained beamformer suppressed all three signals including the desired one, although the location error of the desired signal was very small. The output SINR was  $-6.7$  dB, which indicates that the point-constrained adaptive beamformer is of no practical value in most near-field applications. Fig. 6(b), in contrast, illustrates that the proposed regionally constrained beamformer was able

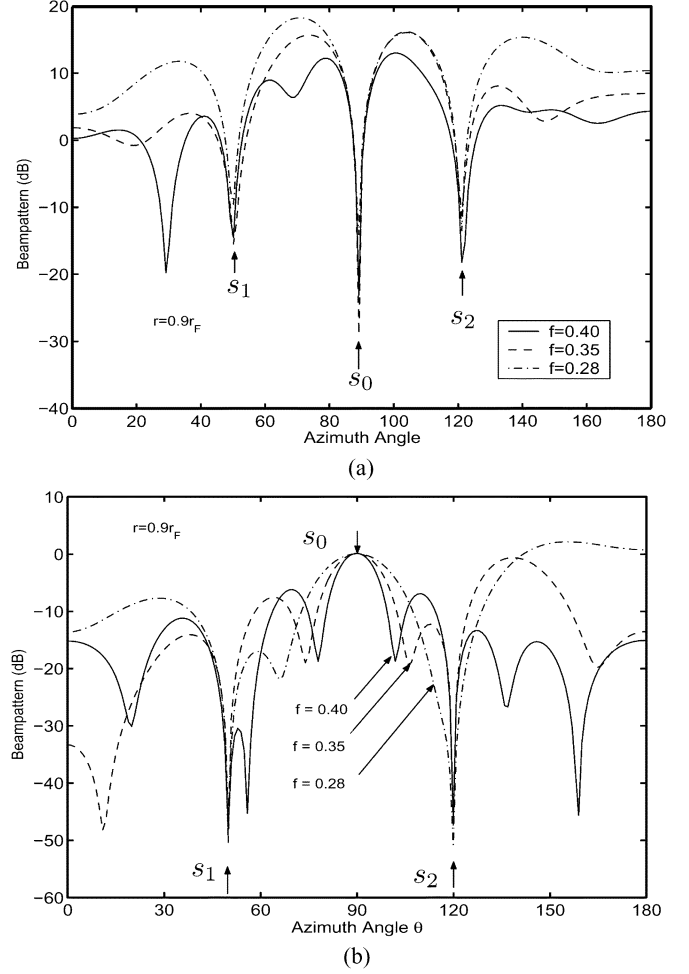


Fig. 6. Beampatterns of the near-field adaptive beamformers with location errors. The presumed focal point is  $\mathbf{x}_F = (r_F, 90^\circ, 90^\circ)$ . The desired signal  $s_0$  is off the focal point at  $(0.9r_F, 88^\circ, 90^\circ)$ . The interfering signals are  $s_1$  and  $s_2$  located at  $(r_F, 50^\circ, 90^\circ)$  and  $(r_F, 120^\circ, 90^\circ)$ , respectively. (a) Point-constrained beamformer. (b) Regionally constrained beamformer.

to preserve the desired signal with unit gain while placing deep nulls at the interfering signal locations. It achieved 25.6 dB SINR at the output. Similar performances were obtained when the desired signal was located at any point within the constrained region, including the presumed focal point. The results shown in Fig. 6 are consistent with those in Fig. 3.

The second example demonstrates the advantage of the proposed beamformer in distance discrimination compared to the fixed near-field beamformer. In this experiment, a total of four signals were used with the first three signals  $s_0$ ,  $s_1$  and  $s_2$  being the same as those in Fig. 6. Another interfering signal  $s_3$  was added at location  $(15r_F, 90^\circ, 90^\circ)$ , directly behind the desired signal  $s_0$ . All four signals were received with 20 dB power at the array center. They were uncorrelated and band-limited to  $B$ . The regionally constrained beamformer was adapted at the presence of the four signals plus background noise and the converged beampatterns were evaluated at the semi-circles with radii  $r = r_F$  and  $r = 15r_F$ , respectively, as shown in Fig. 7(a). The solid line for  $r = 15r_F$  shows that the beamformer suppressed the interference  $s_3$  by 22 dB. Note that this attenuation was achieved by the adaptive beamformer only—the attenuation

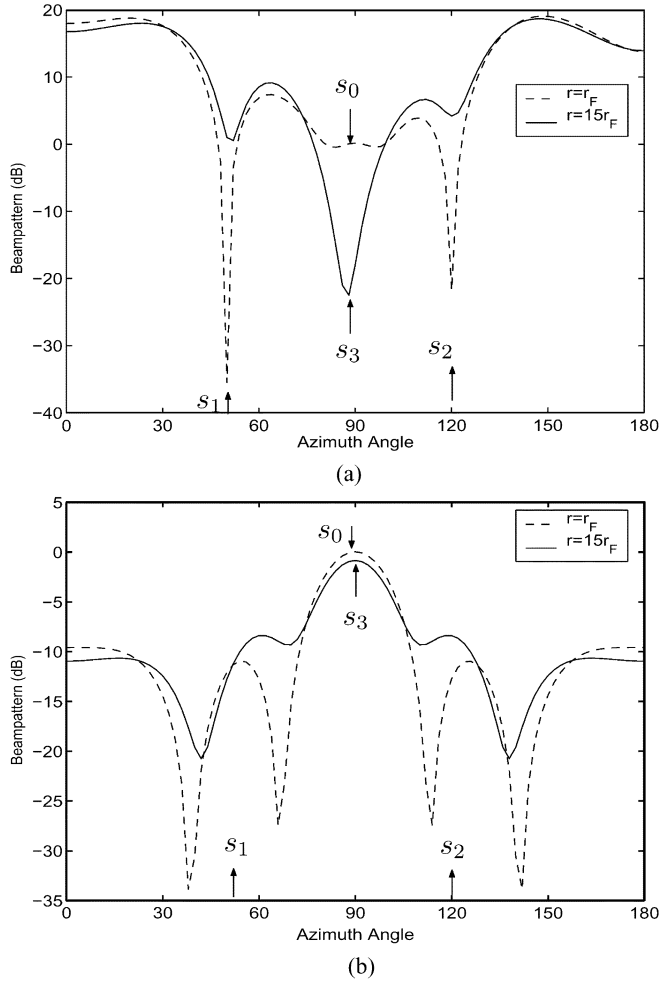


Fig. 7. Distance discrimination of the near-field beamformers. The signals  $s_0$ ,  $s_1$  and  $s_2$  are the same as those in Fig. 6. The additional interfering signal  $s_3$  is at  $(15r_F, 90^\circ, 90^\circ)$ , directly behind the desired one  $s_0$ . (a) Regionally constrained adaptive beamformer. (b) Fixed beamformer.

by propagation was not included. The dashed line for  $r = r_F$  shows that the desired signal was passed with unit gain while  $s_1$  and  $s_2$  were suppressed by the deep nulls. The proposed beamformer achieved an array gain of 15.7 dB and a white noise gain of  $G_w = -7.3$  dB. Meanwhile, the beampatterns of the fixed beamformer were also evaluated at the same two semi-circles and shown in Fig. 7(b). The fixed beamformer could not suppress the interference signals adaptively by placing deep nulls at their locations. The interfering signal  $s_3$  was passed with almost no attenuation. The array gain was only 4.9 dB and the white noise gain was  $G_w = -6.4$  dB. If a soft constraint was placed at the far field signal during the optimization process as proposed in [31], the resulting fixed beamformer improved its distance discrimination at the cost of a reduced gain for the desired signal and a reduced white noise gain. In the four signal scenario, the soft-constrained fixed beamformer obtained an array gain of 5.8 dB and a white noise gain of  $G_w = -12.9$  dB. The proposed regionally constrained beamformer achieved nearly 10 dB higher array gain with a better white noise gain. The advantage of the proposed beamformer in distance discrimination is clearly demonstrated.

### C. Performance in Reverberant Environment

The proposed near-field robust adaptive beamforming method has been applied to a practical microphone array design to demonstrate its performance in reverberant environments. A 17-element nested array was used to cover the speech frequency band of [300, 3400] Hz. They were grouped into three subarrays covering the three subbands  $B_1 = [300, 850]$  Hz,  $B_2 = [850, 1700]$  Hz, and  $B_3 = [1700, 3400]$  Hz with sampling frequencies being  $F_{S1} = 2$  kHz,  $F_{S2} = 4$  kHz, and  $F_{S3} = 8$  kHz, respectively. Therefore, the normalized frequency of the lowest subband was  $[0.15, 0.425]$  and that of the two higher subbands was  $[0.2125, 0.425]$ . The subarrays each had nine elements uniformly spaced at 20.0 cm, 10.0 cm, and 5.0 cm, respectively, which are the half wavelength of the high frequency edge of the corresponding band. The subarray elements were super-imposed and harmonically nested resulting in a total of 17 elements. The multirate subband beamforming technique [14] was then employed with three subband robust adaptive beamformers designed using the proposed regionally constrained near-field beamforming method. The presumed focal point was  $\mathbf{x}_F = (1.0 \text{ m}, 90^\circ, 90^\circ)$ . The constrained distance was  $\Delta r = 0.2r_F$  or equivalently from 0.8 m to 1.2 m. The constrained azimuth angles  $\Delta\theta$  were  $16^\circ$  for the low subband beamformer,  $8^\circ$  for the middle subband beamformer, and  $4^\circ$  for the high subband beamformer. All subband beamformers used  $K = 25$  taps thus, each having  $N = 225$  degrees of freedom. The designed subband beamformers used 112, 89, and 73 linear constraints, respectively.

The reverberant room had a size of 5.0 m  $\times$  4.0 m  $\times$  3.0 m. The nested array was located along a wall at a height of 1.2 m above the floor. The reverberation of the room was simulated by the image model [36] with the reflection coefficients of the walls being 0.8 and those of the ceiling and floor being 0.6. The reverberation time of the simulated room was approximately  $T_{60} \approx 280$  ms, which is typical for realistic office rooms.

A synthesized female speech was used as the target signal located within the constrained region. It was received at the array center with 20 dB power above the background white noise. The reverberation of the signal was generated by convolution of the signal source with the simulated impulse response of the room. No other uncorrelated interference was present in the room. The subband adaptive beamformers were adapted using the NLMS algorithm and their outputs were combined via a synthesis filter. After the convergence, the power spectrum density (PSD) of the combined output were computed, as shown in Fig. 8. The difference between the PSD of the clean target signal  $s_d$  and that of the adaptive beamformer output  $y_{adp}$  indicates the approximate amount of the desired signal cancellation. In the low and middle frequency bands, the signal cancellation was very small although the reverberant interference was larger in these bands. In the high frequency band, the signal cancellation was about 3.0 dB. Good de-reverberation gains were also achieved by the lower subband beamformers. The improvement in SINR was 7.0 dB for the low subband and 5.2 dB for the middle subband. This was because the reverberant signals were virtually originated from far away locations and the lower subband beamformers were able to suppress them with good distance discrimination

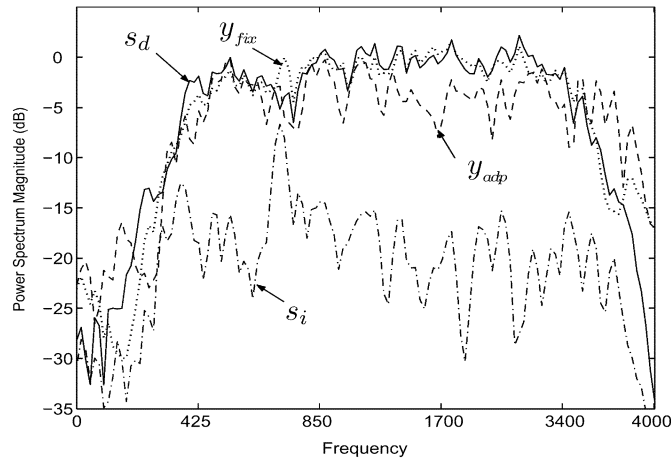


Fig. 8. Input and output PSDs of the subband array beamformers in the reverberant room, where  $s_d$  indicates the desired signal input,  $s_i$  the reverberant interfering input, and  $y_{fix}$  is the output of the fixed beamformer optimized with the far field isotropic noise field,  $y_{adp}$  is the output of the dynamically adaptive beamformers designed by the proposed method.

obtained by the larger subarray sizes; while the constrained distance region of 0.8 m to 1.2 m was close to the far field of the high subband array whose size was only 0.4 m, thus its distance discrimination was limited. Since the reverberant interference is dominant in the lower frequency bands, the overall quality of the beamformer output was improved over the reverberant speech and the signal cancellation was hardly noticeable in subjective listening tests. As a comparison, subband fixed beamformers were also designed for the same nested array with the same three subbands using the optimization method described in Section IV-A. The PSD of the compound fixed beamformer output is also plotted in Fig. 8. The PSD of the fixed beamformer does not exhibit signal cancellation. Instead, it has slightly higher power at some frequencies than the desired signal mainly due to the leakage of the reverberant interference in the output. The peak at which the arrow points clearly shows the effect of the reverberant interference.

The dereverberation performance of our near-field robust adaptive beamformer is also comparable to the one reported in [28], where two reflection boards were arranged in a real room experiment and the four-element far field robust adaptive beamformer had an overall signal cancellation of 2 dB. It was also shown there that the conventional far field nonrobust adaptive beamformer had serious signal cancellation up to 10 dB. With near-field adaptive beamforming (regionally constrained or point-constrained), this was the case only for the high subband array which had poor distance discrimination. It is noted that the good distance discrimination in the lower frequency subband beamformers helped to suppress the reverberant interference and prevented the desired signal cancellation.

## V. CONCLUSION

In this paper, we have proposed a robust regionally constrained LCMV method for near-field adaptive beamforming based on the fact that the eigen-structure of near-field signals with a broad frequency band and over a spatial region can be sufficiently approximated by its low rank subspace represen-

tation. A systematic design method has been developed for the design of the linear constraints which filter on this signal subspace and achieve accurate control of the beamformer responses over the specified region and frequency band. The designed near-field beamformer is dynamically adaptive to the changing environment with robustness against large distance and DOA errors. We have shown, via a nine-element linear array example, that the proposed beamformer is able to tolerate a distance error as large as  $\pm 32\%$  of the presumed radial distance and the DOA error as large as  $\pm 20^\circ$ . Meanwhile, the proposed method also improves distance discrimination of the near-field beamformer without additional constraints. In the scenario where the interfering signal is located at different distances but with the same DOA as the desired signal, the nine-element array beamformer is able to suppress the interfering signal by more than 20 dB without harming the robustness of the beamformer. The proposed method has also been applied to subband adaptive beamformers of a 17-element nested array in reverberant rooms. The results have demonstrated that the distance discrimination of the near-field beamformers improves the de-reverberation gain and reduces the desired signal cancellation.

Other significant advantages of the proposed method include its direct time domain real arithmetic implementation, low computational complexity, and no restrictions on the presence or absence of the desired signals during the data adaptation.

## ACKNOWLEDGMENT

The authors would like to thank the anonymous reviewers and the guest editor for their constructive comments and suggestions which helped greatly in improving the quality of the paper.

## REFERENCES

- [1] D. H. Johnson and D. E. Dudgeon, *Array Signal Processing: Concepts and Techniques*. Englewood Cliffs, NJ: Prentice-Hall, 1993.
- [2] H. Cox, R. M. Zeskind, and M. H. Owen, "Robust adaptive beamforming," *IEEE Trans. Acoust., Speech, Signal Processing*, vol. ASSP-35, pp. 1365–1376, Oct. 1987.
- [3] B. D. Van Veen and K. M. Buckley, "Beamforming: A versatile approach to spatial filtering," *IEEE ASSP Mag.*, pp. 4–24, Apr. 1988.
- [4] J. C. Chen, R. E. Hudson, and K. Yao, "Maximum-likelihood source localization and unknown sensor location estimation for wideband signals in the near-field," *IEEE Trans. Signal Processing*, vol. 50, pp. 1843–1854, Aug. 2002.
- [5] J. G. Ryan, "Criterion for the minimum source distance at which plane-wave beamforming can be applied," *J. Acoust. Soc. Amer.*, vol. 104, no. 1, pp. 595–598, July 1998.
- [6] R. A. Kennedy, T. D. Abhayapala, and D. B. Ward, "Broadband nearfield beamforming using a radial beampattern transformation," *IEEE Trans. Speech Audio Processing*, vol. 46, pp. 2147–2156, Aug. 1998.
- [7] S. E. Nordholm, V. Rehbock, K. L. Tee, and S. Nordebo, "Chebyshev optimization for the design of broadband beamformers in the near-field," *IEEE Trans. Circuits Syst. II*, vol. 45, no. 1, pp. 141–143, Jan. 1998.
- [8] W. Täger, "Near-field superdirectivity (NFSD)," in *Proc. IEEE ICASSP*, vol. 4, May 1998, pp. 2045–2048.
- [9] C. Marro, Y. Mahieux, and K. U. Simmer, "Analysis of noise reduction and dereverberation techniques based on microphone arrays with post-filtering," *IEEE Trans. Speech Audio Processing*, vol. 6, pp. 240–259, May 1998.
- [10] M. Dahl and I. Claesson, "Acoustic noise and echo canceling with microphone array," *IEEE Trans. Veh. Technol.*, vol. 48, pp. 1518–1526, Sept. 1999.
- [11] J. G. Ryan and R. A. Goubran, "Array optimization applied in the near-field of a microphone array," *IEEE Trans. Speech Audio Processing*, vol. 8, pp. 173–176, Mar. 2000.

- [12] —, "Application of near-field optimum microphone arrays to hands-free mobile telephony," *IEEE Trans. Veh. Technol.*, vol. 52, pp. 390–400, Mar. 2003.
- [13] M. S. Branstein and D. B. Ward, "Cell-based beamforming (CE-BABE) for speech acquisition with microphone arrays," *IEEE Trans. Speech Audio Processing*, vol. 8, pp. 738–743, Nov. 2000.
- [14] Y. R. Zheng, R. A. Goubran, and M. El-Tanany, "Experimental evaluation of a nested microphone array with adaptive noise cancellers," *IEEE Trans. Instrum. Meas.*, vol. 53, pp. 777–786, June 2004.
- [15] A. B. Gershman, "Robust adaptive beamforming in sensor arrays," *Int. J. Electron., Commun.*, vol. 53, no. 3, pp. 305–314, Dec. 1999.
- [16] K. M. Buckley, "Spatial/spectral filtering with linearly-constrained minimum variance beamformers," *IEEE Trans. Acoust., Speech, Signal Processing*, vol. ASSP-35, pp. 249–266, Mar. 1987.
- [17] Y. R. Zheng, R. A. Goubran, and M. El-Tanany, "On constraint design and implementation for broadband adaptive array beamforming," in *Proc. IEEE ICASSP*, vol. 3, Orlando, FL, May 2002, pp. 2917–2920.
- [18] M. W. Hoffman and K. M. Buckley, "Robust time-domain processing of broadband microphone array data," *IEEE Trans. Speech Audio Processing*, vol. 3, pp. 193–203, May 1995.
- [19] M. H. Er and A. Cantoni, "Derivative constraints for broad-band element space antenna array processors," *IEEE Trans. Acoust., Speech, Signal Processing*, vol. ASSP-31, pp. 1378–1393, Dec. 1983.
- [20] G. L. Fudge and D. A. Linbarger, "Spatial blocking filter derivative constraints for the generalized sidelobe canceller and MUSIC," *IEEE Trans. Signal Processing*, vol. 44, pp. 51–61, Jan. 1996.
- [21] J.-L. Yu and C.-C. Yeh, "Generalized eigenspace-based beamformers," *IEEE Trans. Signal Processing*, vol. 43, pp. 2453–2461, Nov. 1995.
- [22] S.-J. Yu and J.-H. Lee, "Efficient eigenspace-based array signal processing using multiple shift-invariant subarrays," *IEEE Trans. Antennas Propagat.*, vol. 47, pp. 186–194, Jan. 1999.
- [23] S. A. Vorobyov, A. B. Gershman, and Z.-Q. Luo, "Robust adaptive beamforming using worst-case performance optimization: A solution to the signal mismatch problem," *IEEE Trans. Signal Processing*, vol. 51, pp. 313–324, Feb. 2003.
- [24] S. Shahbazzpanah, A. B. Gershman, Z.-Q. Luo, and K. M. Wong, "Robust adaptive beamforming for general-rank signal models," *IEEE Trans. Signal Processing*, vol. 51, pp. 2257–2269, Sep. 2003.
- [25] B. D. Van Veen, "Minimum variance beamforming with soft response constraints," *IEEE Trans. Signal Processing*, vol. 39, pp. 1964–1972, Sept. 1991.
- [26] F. Qian and B. D. Van Veen, "Quadratically constrained adaptive beamforming for coherent signals and interference," *IEEE Trans. Signal Processing*, vol. 43, pp. 1890–1900, Aug. 1995.
- [27] M. M. Sondhi and G. W. Elko, "Adaptive optimization of microphone arrays under a nonlinear constraint," in *Proc. ICASSP*, vol. 2, Tokyo, Japan, Apr. 1986, pp. 981–984.
- [28] O. Hoshuyama, A. Sugiyama, and A. Hirano, "A robust adaptive beamformer for microphone arrays with a blocking matrix using constrained adaptive filters," *IEEE Trans. Signal Processing*, vol. 47, pp. 2677–2684, Oct. 1999.
- [29] W. Herboldt and W. Kellermann, "Efficient frequency-domain realization of robust generalized sidelobe cancellers," in *IEEE Proc. 4th Workshop Multimedia Signal Processing*, Oct. 2001, pp. 377–382.
- [30] D. B. Ward, "Mixed nearfield/farfield beamforming: A new technique for speech acquisition in a reverberant environment," in *IEEE ASSP Workshop Applications Signal Processing Audio Acoustics*, Oct. 1997.
- [31] J. G. Ryan and R. A. Goubran, "Optimum near-field performance of microphone arrays subject to a far-field beam pattern constraint," *J. Acoust. Soc. Amer.*, pt. 1, vol. 108, no. 5, pp. 2248–2255, Nov. 2000.
- [32] N. Ahmed and K. R. Rao, *Orthogonal Transforms for Digital Signal Processing*. New York: Springer-Verlag, 1975, ch. 9.1, pp. 200–205.
- [33] D. Slepian and H. O. Pollak, "Prolate spheroidal wave functions, Fourier analysis and uncertainty—I," *Bell Syst. Tech. J.*, vol. 40, no. 1, pp. 43–64, Jan. 1961.
- [34] S. Haykin, *Adaptive Filter Theory*, 3rd ed. Upper Saddle River, N.J.: Prentice Hall, 1996.
- [35] J. G. Proakis and D. G. Manolakis, *Digital Signal Processing: Principles, Algorithms, and Applications*, 3rd ed. Englewood Cliffs, N.J.: Prentice Hall, 1996, ch. 8.
- [36] J. B. Allen and D. A. Berkley, "Image method for efficiently simulating small room acoustics," *J. Acoust. Soc. Amer.*, vol. 65, no. 4, pp. 943–950, Apr. 1979.



**Yahong Rosa Zheng** received the B.S. degree from the University of Electronic Science and Technology of China, Chengdu, in 1987, the M.S. degree from Tsinghua University, Beijing, China, in 1989, and the Ph.D. degree from Carleton University, Ottawa, ON, Canada, in 2002, all in electrical engineering.

From 1989 to 1994, she was a Senior Member of Scientific Staff with the Peony Electronic Group, Beijing, China. From 1994 to 1997, she held positions with GPS Solutions at Sagem Australasia Pty. Ltd., Sydney, Australia, and Polytronics Pty. Ltd., Toronto, ON, Canada. Currently, she is an NSERC Postdoctoral Fellow with the Department of Electrical and Computer Engineering at the University of Missouri, Columbia. Her research interests include digital signal processing algorithms, array signal processing, and channel estimation and modeling for wireless communications.



**Rafik A. Goubran** (M'00) received the B.Sc. and M.Sc. degrees in electrical engineering from Cairo University, Cairo, Egypt, in 1978 and 1981, respectively, and the Ph.D. degree in electrical engineering from Carleton University, Ottawa, ON, Canada, in 1986.

In January 1987, he joined the Department of Systems and Computer Engineering at Carleton University where he is now Professor and Chair. He was involved in several research projects with industry and government organizations including Nortel Networks, Mitel Networks, Bell Canada, NEC Corporation, the Department of National Defense (DND), and the National Research Council of Canada (NRC), Ottawa. His research interests include digital signal processing (DSP) and its applications in audio and biomedical engineering, voice transmission over IP networks (VoIP), noise and echo cancellation, and beamforming using microphone arrays.



**Mohammed El-Tanany** received the B.Sc. and M.Sc. degrees in electrical engineering in 1974 and 1978, respectively, both from Cairo University, Giza, Egypt, and the Ph.D. degree in electrical engineering from Carleton University, Ottawa, ON, Canada, in 1983.

He worked with the Advanced Systems division of Miller Communications, Kanata, ON, Canada, from 1982 to 1985 with principal involvement in the research and development of digital transmission equipment for mobile satellite type of applications and also for VHF airborne high-speed down links. He joined Carleton University in 1985. He is currently a Professor with the Department of Systems and Computer Engineering. His research activities are mainly in the areas of digital wireless communications with emphasis on the transmission subsystems from a hardware design and algorithm design points of view, Digital TV and Digital Audio Broadcasting systems, experimental characterization and empirical modeling of the wireless communications channels and Digital TV channels in various environments and at various frequency bands.